ELECTROCHEMICAL DEGRADATION OF NAPROXEN FROM WATER BY ANODIC OXIDATION WITH MULTIWALL CARBON NANOTUBES GLASSY CARBON ELECTRODE

Short tittle: **ELECTROCHEMICAL OXIDATION OF NAPROXEN BY CARBON NANOTUBEs AT CONSTANT POTENTIAL**

Eva Díaz, Sonia Stożek, Yolanda Patiño, Salvador Ordóñez

Department of Chemical and Environmental Engineering,

University of Oviedo, Faculty of Chemistry, Julián Clavería s/n, 33006 Oviedo, Spain

E-mail: diazfeva@uniovi.es

Abstract

Naproxen (NPX) degradation was investigated by anodic oxidation both at constant potential and by cyclic voltammetry (CV), using this last technique for optimizing reaction conditions and catalyst properties. Three MWCNTs-promoted electrodes were used (MWCNT, MWCNT-COOH and MWCNT-NH_2) and a two steps oxidation process was observed in all the cases. At the optimized conditions (volume of MWCNT = 15 μL), the influence of the scan rate indicates the diffusion – adsorption control of the process. Likewise, the kinetic study of NPX degradation at fix potential, considering two different stirring speeds (250 and 500 rpm), indicates that degradation rate increases with the stirring speed. After 20 h, NPX is degraded even an 82.5 %, whereas the mineralization reaches almost 70 % as it was obtained from TOC analysis.

pH effect was also analysed, in the range 5-11, observing a positive effect at low pH.

Concerning the surface chemistry of the electrode, MWCNT-NH_2, with the highest isoelectric point (4.70), is the most promising material due to the improved interactions with the reactant. From these observations, a pathway is proposed, which includes two steps of electrochemical oxidation followed by subsequent oxidation steps, until mineralization of the NPX, attributed mainly to active chlorine species and ·OH.

Keywords: anodic oxidation, degradation pathway, functionalization, multiwall carbon nanotubes, Naproxen

INTRODUCTION

Nonsteroidal anti-inflammatory drugs (NSAIDs), belonging to pharmaceuticals and personal care products (PPCPs), are widely used for the treatment of headaches, arthritis, spondylitis, etc. and even in cancer treatments (Wojcieszyńska *et al*. 2014; Coria *et al*. 2016). In addition, many of them are non-prescription drugs being more accessible, thus, their consumption is of several tons per year in developed countries (Loss *et al*. 2013; Wojcieszyńska *et al*. 2014). Among NSAIDs, Naproxen (NPX) is one of the most commonly used (Ding *et al*. 2017). Because of the increasing consumption of NSAIDs, direct disposal of these compounds into aquatic systems has increased their presence in rivers and groundwater. NSAIDs are polar, so soluble in water, and its removal efficiency in wastewater treatment plants (WWTP) is just around 20% (Coria *et al*. 2016). Concretely, in the case of Naproxen (NPX), the removal efficiency in WWTP reaches values lower than 15%.

Loss *et al*. (2013) found the NPX presence in 69 of the 100 studied European rivers, from 27 different countries, in concentrations higher than 2.027 $ng \cdot L^{-1}$. Although, NSAIDs concentration is usually low in water ($ng \cdot L^{-1}$ or $\mu g \cdot L^{-1}$), the continuous exposure to these compounds may have adverse effects on living organisms; gastrointestinal and renal effects were described for NPX (Ding *et al*. 2017).

The most studied methods of removing NPX from water and wastewater are: adsorption (Katsigiannis *et al*. 2015), biodegradation (Wojcieszyńska *et al*. 2014; Ding *et al*. 2017) and photodegradation (Štrbac *et al*. 2018). In the case of adsorption, removal efficiency values from 50 to 100% can be obtained depending on the adsorbent. For example, adsorption onto granular activated carbon removes 65.6% of NPX (Katsigiannis *et al*. 2015). The main drawback of the adsorption is the pollutant transference from the liquid to a solid phase (adsorbent), so a further treatment for the pollutant removal is necessary (Chin *et al*. 2014). Biodegradation techniques present the inconvenience of the long time needed for an effective degradation, reaching even several days (Ding *et al*. 2017). Photodegradation techniques have

demonstrated to be an effective way to degrade these kind of pollutants, with removal efficiencies close to 90% for ozonation, or around 100% for photolysis. Nevertheless, the byproducts are usually found to be more toxic than the parent compounds.

In the search for a green-technology for NPX removal, the electrochemical oxidation is an interesting alternative, since in the mineralization of the pollutants, it does not use any external oxidizing agent. The only requirement is the suitable electrode to achieve the pollutant oxidation (Chin *et al*. 2014).

In this way, chemically modified electrodes have been used to boost the electron transfer for the electro-oxidation of organic pollutants (Ardelean *et al*. 2016). Both carbon nanotubes (CNTs) and multiwall carbon nanotubes (MWCNTs), have been widely used to improve electrode performance because of their exceptional features: high electrical conduction, high surface area, chemical stability and good hydrophobicity. Carbon nanotubes present several advantages; they produce a decrease in the overpotential of electrochemical oxidation reactions, as well as an increase in the electrode active surface area, and provide greater electrode stability.

The performance of three kinds of MWCNT (non- functionalized (MWCNT), functionalized with carboxylic (MWCNT-COOH) and amine (MWCNT-NH_2) groups) for the electrochemical degradation of NPX was studied in this work. These materials were already used in the electrochemical oxidation of both NAL and MPET, using cyclic voltammetry for optimizing the operation conditions (Patiño *et al*. 2017; Patiño *et al*. 2018). This technique allows a systematic study of the electrochemical oxidation, as well as identifying the effect of both electrode properties and operation conditions. However, the novelty of this work is double, on one side, the use of Naproxen as reactant and the study of the influence of both the pH, and the functionalization of the MWCNTs surface; and on the other hand, the effect of the stirring speed on the degradation of NPX.

Naproxen electrochemical degradation by cyclic voltammetry was already study by Chin (2014) with platinum nanoparticles supported both on fluorine tin oxide (FTO) and MWCNTs/FTO, thus the study was focused on the role of Pt. Likewise, naproxen detection by CV using MWCNTs modified electrode was researched (Montes *et al*. 2016). Taskhourian (2014) studied the effect of the incorporation of both, ZnO nanoparticles and MWCNTs in the electrode for the NPX electrooxidation. Thus, a deep study of the MWCNTs and its functionalization on the NPX removal is, to the best of our knowledge, unexplored. What is more, the role of the functionalization and the influence of pH for each functional group is addressed here for the first time. Furthermore, this work studies the influence of stirring speed, proposing a kinetic and a degradation pathway based on the detected by-products.

MATERIALS AND METHODS

Reagents and materials

Naproxen (NPX) was purchased from Sigma-Aldrich with a purity ≥ 98%. All reactants used in the buffer solutions were from Sigma-Aldrich and in analytical grade. Phosphate buffer (PBS) solutions were prepared by mixing the corresponding amount of sodium chloride (NaCl), potassium chloride (KCl), potassium phosphate monobasic (KH_2PO_4) and sodium phosphate dibasic (Na_2HPO_4).

Three different MWCNT manufactured by DropSense have been checked: non-functionalized MWCNT, MWCNT functionalized with -COOH groups (MWCNT-COOH) and with -NH_2 groups (MWCNT-NH_2), whose main properties were determined in previous works (Patiño *et al*. 2017; Patiño *et al*. 2018).

Preparation of the different MWCNT modified GCEs.

GCE electrodes were modified following the procedure optimized in our previous work (Patiño *et al*. 2017). GCE was polished with aluminium slurry and rinsed with distilled water prior to their modification. After drying at room temperature, different volumes (5-20 μL) of a MWCNT

106 suspension in dimethylformamide (DMF) (concentration of 0.25 $g \cdot L^{-1}$) were deposited on the
107 electrode surface and dried at room temperature before electrochemical test.

108 **Electrochemical measurements and analytical instrument**

109 Cyclic voltammograms were performed using a Zahner XPOT Potentiostat in order to
110 characterize the system, step prior to the degradation study, since it allows an optimization of
111 the variables that affect the degradation. A conventional three electrode cell was used with
112 bare or modified glassy carbon electrodes (GCE) as working electrode, saturated calomel (SCE)
113 as reference electrode and platinum (Pt) as auxiliary electrode.

114 Degradation test were carried out at constant potential, using MWCNT-GCE as anode and
115 platinum electrode as cathode. In all cases, the solution was deoxygenated before each
116 measurement in order to prevent any oxygen interferences in the obtained signals.

117 NPX samples obtained in the degradation tests were analysed and quantified by High Pressure
118 Liquid Chromatography (HPLC) using an Agilent 1200 with an UV-VIS detector and a 150 mm
119 Zorbax SB-Aq column. The reaction products obtained were determined by high performance
120 liquid chromatography with mass spectrometry detector (LC–MS), using a UPLC Agilent
121 6460.2.3. NPX degradation was confirmed by total organic carbon (TOC) measurements, which
122 were carried out using a TOC analyser (Shimadzu TOC-VCSH).

123

124 **RESULTS AND DISCUSSION**

125 **Voltammetric naproxen oxidation on MWCNT-GCE and bare electrode**

126 Figure 1 shows the CV obtained for the naproxen oxidation at MWCNT-GCE, in 19 ppm
127 naproxen and PBS buffer of pH = 7.5 at the scan rate of 50 mV/s and with a stirring speed of
128 500 rpm. Two irreversible oxidation peaks were observed at 0.35 and 0.88 V. In a previous
129 essay on the bare-GCE no peaks were detected at this concentration (19 ppm), whereas not
130 electrochemical signals were observed in the blank experiment (absence of NPX) on the

MWCNT-GCE. Thus, the MWCNT presence improves the electron transfer process and therefore, the naproxen oxidation.

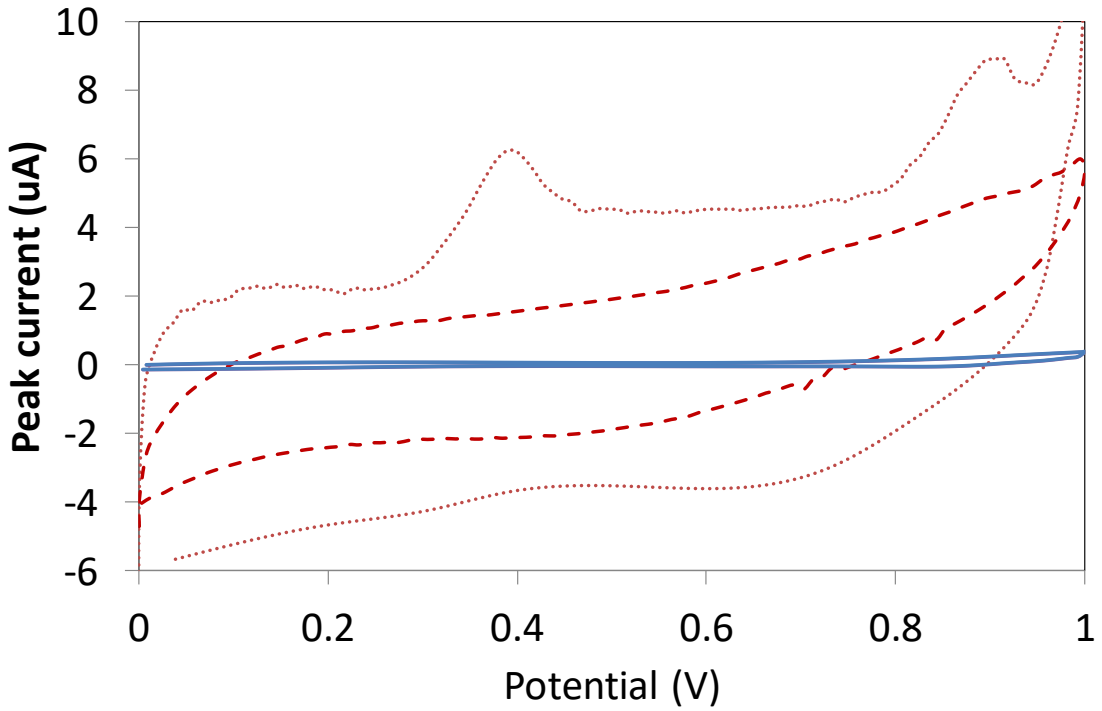

Figure 1. CVs of bare-GCE and MWCNT-GCE as working electrodes in the presence of 19 ppm of NPX at scan rate of 50 mVs^{-1}, pH = 7.5 and stirring speed of 500 rpm. Bare- GCE (—), MWCNT-GCE blank (- - -) and MWCNT-GCE with NPX (····).

Reported works on electroxidation of NPX show both a single irreversible oxidation peak for naproxen, and several works have found the existence of two irreversible oxidation peaks. In the first group, Soltani *et al*. (2018) observed a well defined anodic peak at 0.936 V using a carbon paste electrode modified with activated carbon. Tashkhourian (2014) obtained similar results, in this case on ZnO-MWCNTs electrodes, as well as Ardelean (2016) on a BDD electrode, where a peak at a potential of 0.9 V was detected on a CNF epoxy electrode. In the second group, Montes *et al*. (2016) and Aguilar-Lira *et al*. (2015) found two irreversible oxidation peaks between 0.835-1 and 1.131-1.21 V, where the working electrodes were GCE or modified-GCE and graphite; the reference electrodes were Ag/AgCl/saturated KCl and Ag/AgCl, respectively; and Pt and carbon bar were used as auxiliary electrodes, respectively. Likewise,

Sarhangzadeh (2015) with MWCNT and graphite hybrid electrodes, using a Pt wire as auxiliary and a saturated calomel electrode (SCE) as reference electrodes, obtained an irreversible oxidation peak at around 0.7 V (pH = 7), and a second reversible peak at about 0.4 V. Thus, it is obvious that add to the working electrode, the choose of both the auxiliary and reference electrodes conditioned the potential, being observed similar potential intervals as in our work in the case of using a saturated calomel (SCE) as reference electrode and a platinum (Pt) as auxiliary electrode. In fact, measurements of different reference electrodes versus each other confirm potential shifts of even 400 mV for the CH_3CN at 25 °C (Pavlishchuk and Addison 2000).

Effect of catalyst loading and CV scan rate on NPX oxidation

The effect of the volume of MWCNT to drop on the electrode surface was studied from 5 to 20 μL (Figure 2). When the volume was increased from 5 to 15 μL, the peak current also increased due to the increased amount of MWCNT and as consequence, the increased effective surface area. By increasing the effective surface area, the concentration of NPX on the electrode surface increases, favouring its oxidation. On the other hand, when the volume of MWCNT increases up to 20 μL, the peak current decreased. The same behaviour was already observed in previous works (Jain and Sharma 2012; Patiño *et al*. 2017). So, an intermediate film thickness is necessary to allow degradation, but too thick nanotubes layer promote its instability. For this reason, the optimum amount of MWCNT to drop on the electrode surface is 15 μL.

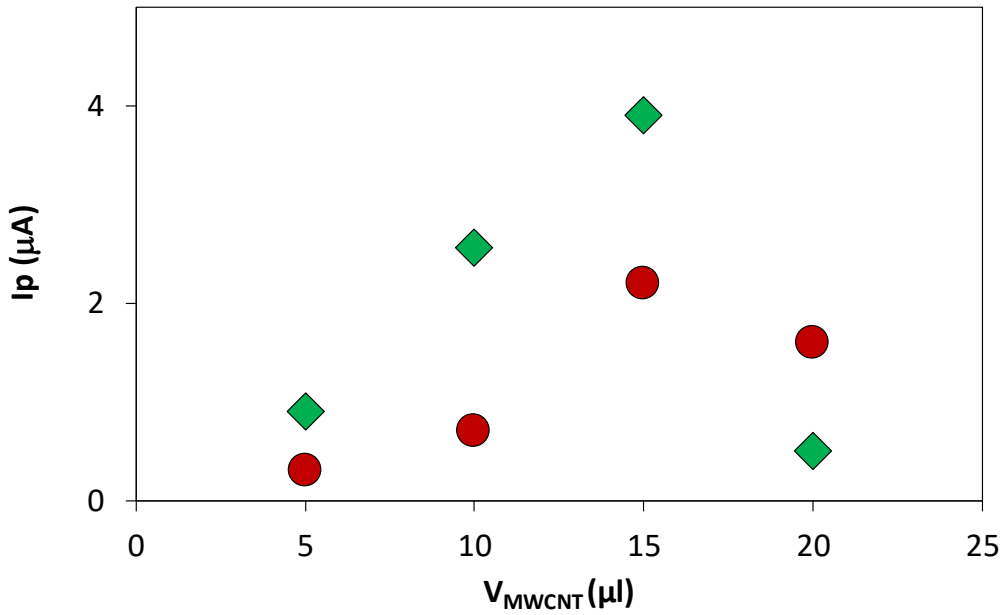

Figure 2. Optimization of the MWCNT volume to drop on the electrode surface. 19 ppm of NPX in PBS at pH 7.5 ◆ Oxidation peak at 0.33 V, and ● Oxidation peak at 0.88 V

Scan rate (SR, ν) influences the rate of adsorption of species on the electrode. By plotting log Ip vs log ν, the process is assumed to be controlled by adsorption when the slope is close to 1.0 and controlled by diffusion if it is close to 0.5. An intermediate slope value indicates that the process is a mixed control: diffusion-adsorption. A linear regression was obtained for both peaks (Figure 3) and the equations can be expressed according to Eq. 1 and Eq. 2.

$$\log Ip = 0.6811 \log \nu - 0.8953 \quad (r^2=0.97) \qquad (1)$$

$$\log Ip = 0.9949 \log \nu - 1.7066 \quad (r^2=0.98) \qquad (2)$$

For the oxidation peak at 0.33 V, the slope of 0.6811 indicates that the process has a mixed control: diffusion-adsorption (Wu *et al.*, 2016). On the other hand, for the oxidation peak at 0.88 V, the slope close to 1.0 confirms that the process is controlled by adsorption (Shin *et al.* 2011). This fact suggest that the electrochemically relevant process consists of two serial reactions of adsorbed species, the first one being faster and therefore more likely to be controlled by mass transfer.

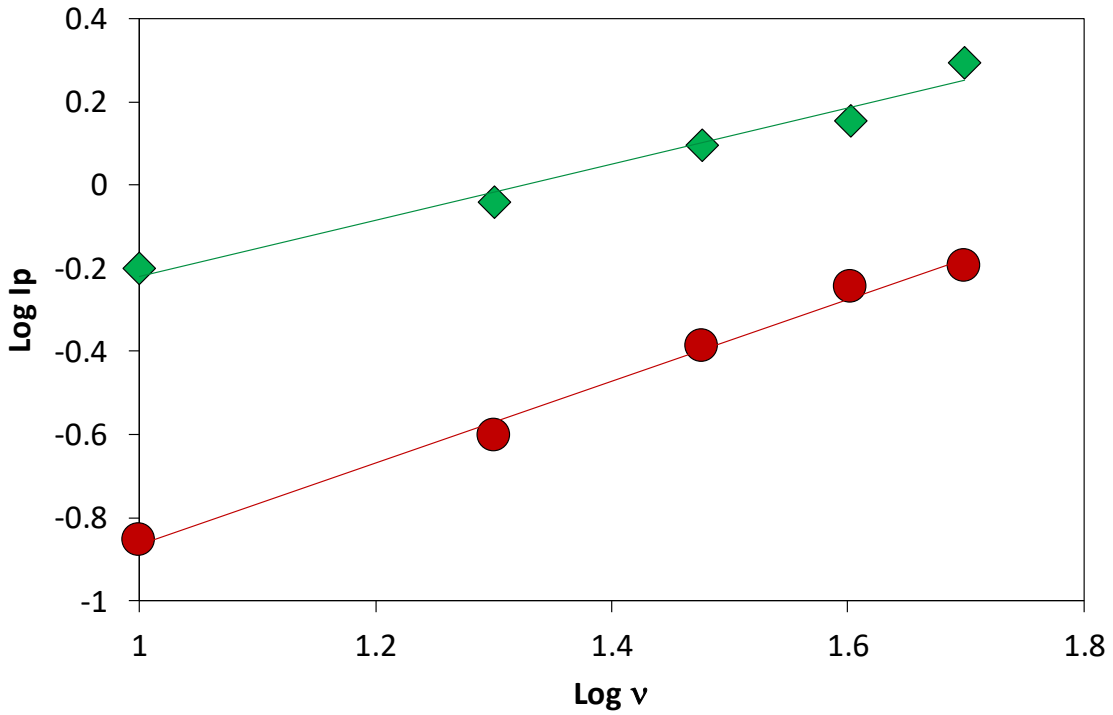

Figure 3. log Ip against log ν. 19 ppm of NPX in PBS at pH 5.0. ◆ Oxidation peak at 0.33 V, and ● Oxidation peak at 0.88 V

NPX degradation on MWCNTs-GCE in a batch reactor at constant potential

Since the practical application of this process to the treatment of NPX-polluted waters require the operation at constant potential, the following set of experiments were performed at batch mode and working at fixed potential.

The degradation of NPX using MWCNT-GCE electrode at fixed potential (1.5V) in a batch reactor, with a total volume of 10 mL and an initial concentration of 19 ppm under stirring at optimal conditions - pH 7.5 and V_{MWCNT}=15 μL -, is shown in Figure 4. Likewise, the effect of stirring speed on the NPX degradation was considered, working at two different stirring rates, 250 and 500 rpm.

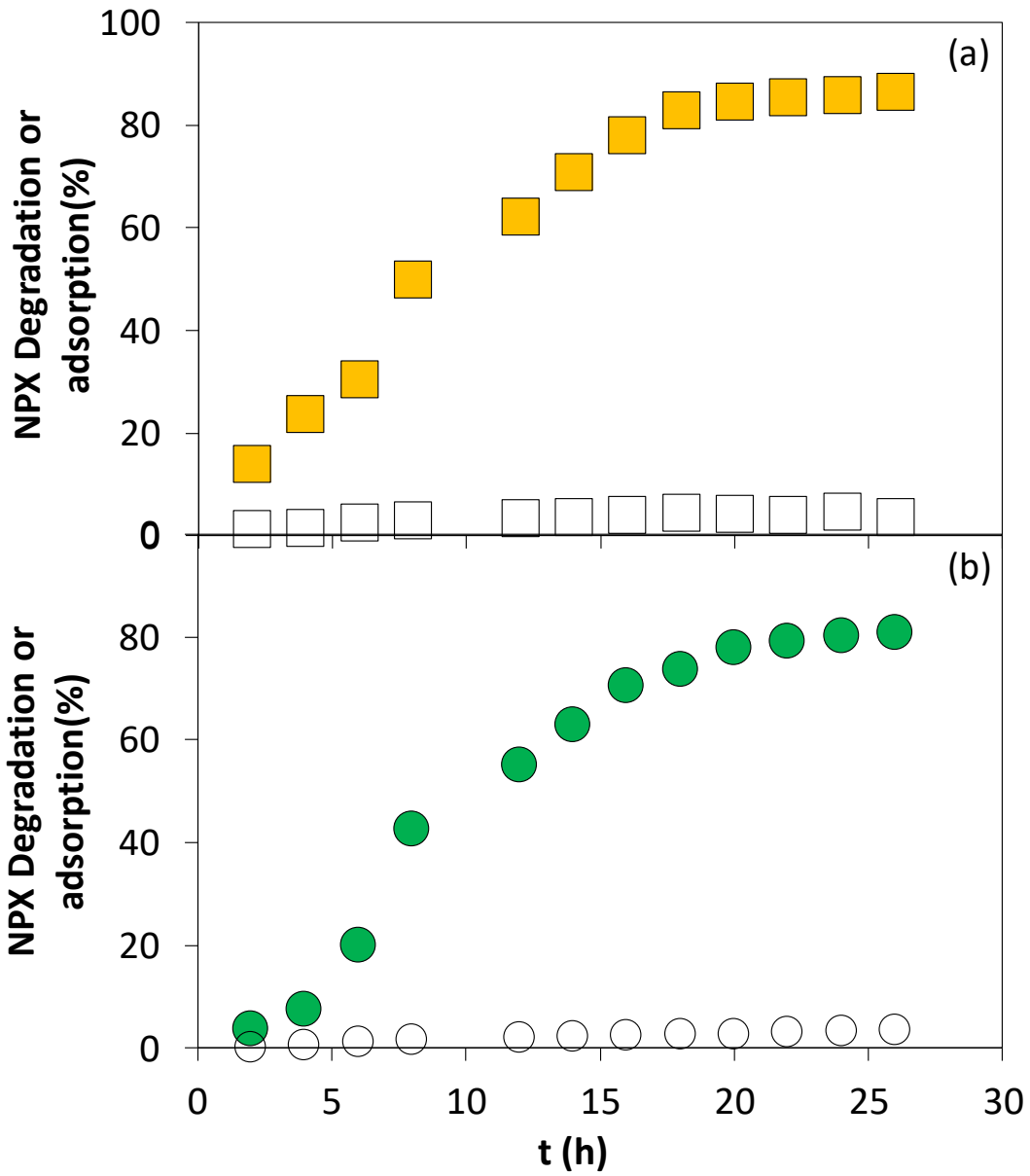

Figure 4. NPX degradation (filled symbol) and NPX adsorbed on the electrode surface (empty symbols) at constant potential (+1.5V) with MWCNT-GCE as anode under stirring: 500 rpm (a) and 250 rpm (b). 19 ppm of NPX in 10 mL of PBS at pH 7.5.

NPX concentration evolution, obtained from HPLC analysis of the NPX solution, reveals that the maximum NPX removal from the water samples, 86.5%, is reached after 22h at 500 rpm. When the stirring speed was reduced by half, the removal efficiency was ≈81%. This fact suggests that stirring speed does not significantly influence the NPX external and internal diffusion from

the solution to electrode surface, as well as its adsorption on it. In both cases, degradation remains constant after 20-22 hours, suggesting saturation of the electrode surface.

NPX adsorption on the electrode could mask the actual degradation value, thus the amount of NPX adsorbed on the electrode surface was quantified in an additional experiment without electrochemical reaction. From Figure 4, it is observed that this amount is lower than 4% of the degradation obtained in both cases – 250 and 500 rpm –. Therefore, the maximum NPX degradation would be 82.5% and 77% for 500 and 250 rpm, respectively.

From NPX concentration is still unknown the actual decontamination potential of the technique, since organic byproducts in the oxidations could be produced. Hence, the total organic carbon (TOC) evolution is showed in Figure 5, together with the C/C_0 ratio. As can be seen, the NPX disappearance is greater than that of TOC. It is due to the presence of byproducts, that have not been completely mineralized and influence on the TOC results. The residual TOC after 20 h is less than 30% at 500 rpm and close to 33% at 250 rpm, which confirm NPX removal. What is more, considering the unreacted NPX in the solution, just about 40 % of the residual TOC corresponds to byproducts of the reaction, which corroborated that TOC does not decrease at the same time than NPX concentration. These results are promising, especially in comparison with those obtained by other techniques. In this way, biological techniques reached a maximum degradation of 80% after 30-35 days (Wojcieszyńska *et al*. 2014; Ding *et al*. 2017) whereas by photocatalytic ones, total degradation of NPX was observed after half an hour on ZnO and TiO_2 materials (Kanakaraju *et al*. 2015; Štrbac *et al*. 2018).

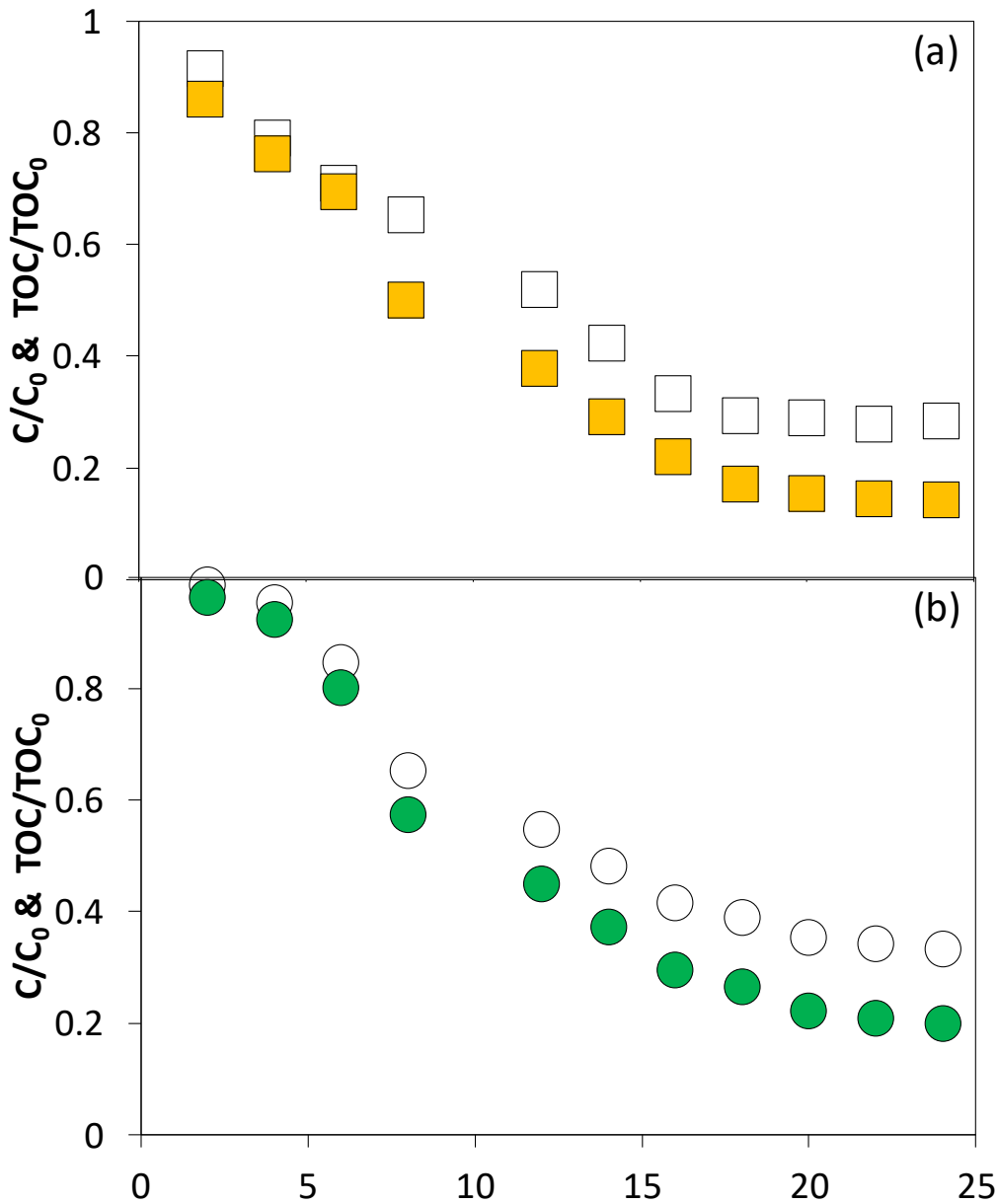

Figure 5. C/C_0 evolution (filled symbol) and TOC/TOC_0 evolution (empty symbols) at constant potential (+1.5V) with MWCNT-GCE as anode under stirring: 500 rpm (a) and 250 rpm (b). 19 ppm of NPX in 10 mL of PBS at pH 7.5.

The NPX concentration with time was fitted to a pseudo-first order kinetic equation, considering data until electrode saturation, (Eq. 3).

$$r_0 = -\frac{dC}{dt} = -k \cdot C \qquad (3)$$

Where C ($mg \cdot L^{-1}$) is the NPX concentration, t is the reaction time (h) and k is the degradation rate constant (h^{-1}).

The experimental results fit perfectly to the proposed model with a correlation coefficient r^2= 0.98, obtaining a degradation constant of 0.10 h^{-1} at 500 rpm and 0.08 h at 250 rpm, thus NPX degradation rate increases with the stirring speed. These results are congruent with the diffusion-adsorption control of the process previously stated, since the mass transfer limitations decrease as the stirring velocity increases.

Effect of pH and functionalization of MWCNTs on the naproxen oxidation

In order to get a deep insight into the effect of the surface into the NPX oxidation, it was investigated in the interval of 5-11 (Figure 6). The pH range was selected from the saturated solubility studies of naproxen in aqueous medium of Kumar *et al*. (2015), where it is observed that the drug solubility at pH lower than 5 was very low.

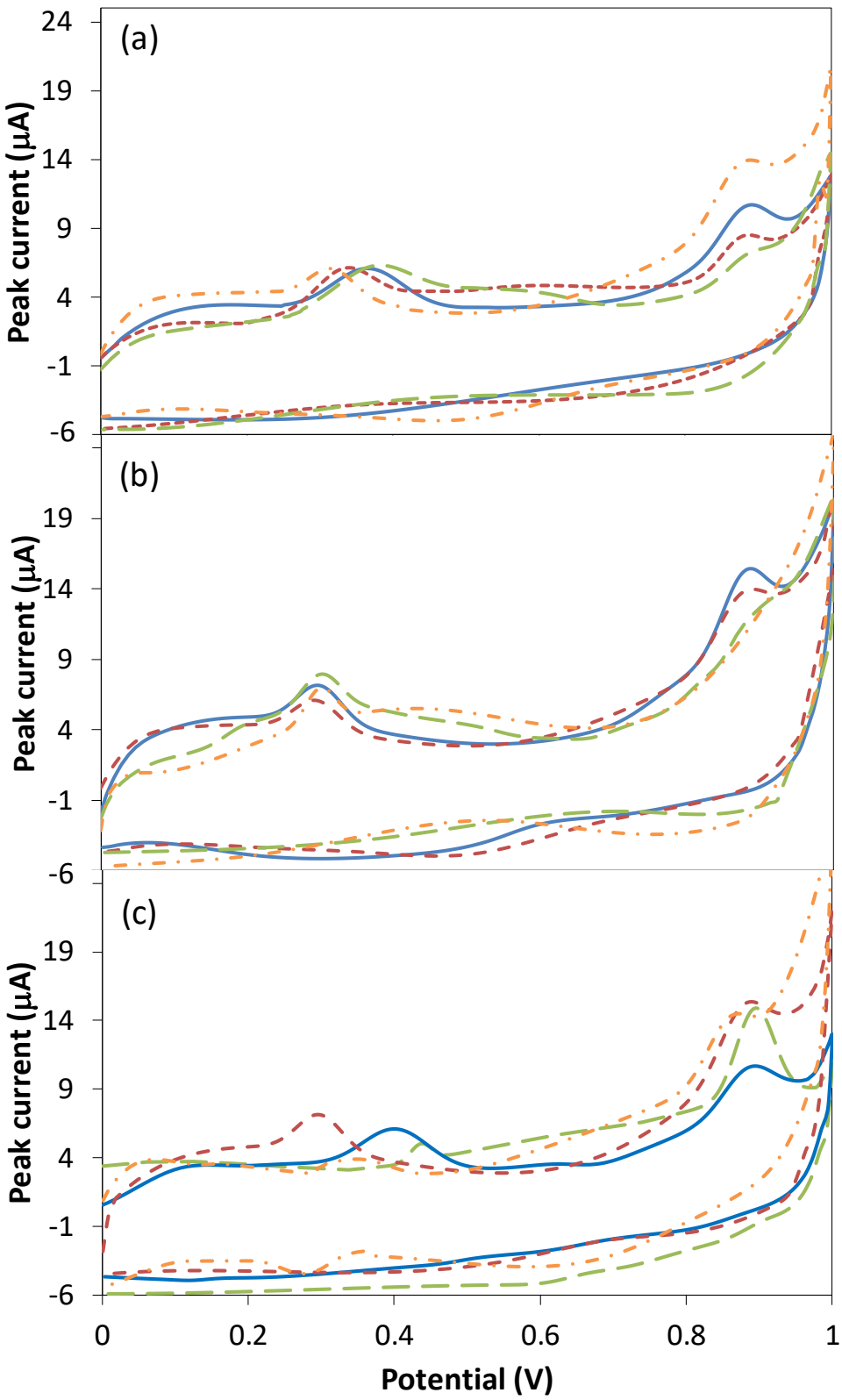

Figure 6. CVs in the presence of 19 ppm of NPX in PBS at different pH and scan rate of 50 mVs^{-1}, using as working electrode: (a) MWCNT, (b) MWCNT-NH_2 and (c) MWCNT-COOH. – –pH 5, — pH 7, -- pH 9 and -·-·- pH 11.

From Figure 6a is observed that the oxidation peak potential shifted, when the pH decreases, to lower values in the interval under study (5-11). This effect is observed in both oxidation peaks, with displacements from 0.37 to 0.33 V and from 0.91 to 0.85 V. Concerning the peak current, the low potential peak decreases in the range 5- 11 pH, thus the NPX oxidation increased at the most acidic pH. The same finding was already reached by Chin (2014) for the oxidation of NPX; what is more, in an experiment without pH control, a decrease in the pH with the reaction extension was observed, pointed out the formation of acidic species. In the case of the high potential peak, the more basic medium seems to favour the oxidation process, although this effect is less marked.

Considering that the pKa of naproxen is 4.12, the molecule presents in the deprotonated form at all pH considered in this work. Likewise, the isoelectric point of the MWCNT is 4.19, so repulsion forces between the negative charged surface and the reactant could occur (Patiño *et al*. 2015). These repulsive forces will increase their intensity with the pH, hence the best performance of pH=5.

Voltamperograms corresponding to NPX oxidation on MWCNT-NH_2 modified electrode are shown in Figure 6b, whereas the corresponding to MWCNT-COOH are shown in Figure 6c. As in the MWCNT electrode, a shift of the peaks potential towards less positive values with the lower pH is observed by MWCNT-NH_2 electrode, although the intervals are narrower (0.27-0.3 V; 0.9-0.87 V). For MWCNT-COOH, the peak potential range is so tight among the different pH that no conclusions could be drawn. The isoelectric points are 4.70 and 0.64 for MWCNT-NH_2 and MWCNT-COOH respectively, thus, the repulsive forces between deprotonated reactive molecule and the surface of the MWCNT-COOH could hinder the extension of the reaction, even at the lowest pH (Patiño *et al*. 2015). Furthermore, for MWCNT-NH_2, at pH=5, which is close to the pKa of NPX, it is observed the highest peak intensity (Ep = 0.27 V), thus the reaction is developed at a largest extent. Concerning the peak at Ep ≈ 0.9 V, it is remarkable the highest peak current in the case of the MWCNT-COOH electrode, that could be consistent

with the formation of an uncharged specie, so its interaction with the negative charged surface of this material could favour the reaction.

Regarding to the other physical-chemical properties of MWCNTs (S_{BET}, V_{meso}, pore width, electrode surface), no relationship was obtained between them and the MWCNTs behaviour, so only isoelectric point influences the results obtained.

The facts previously exposed are congruent with the naproxen oxidation mechanism proposed by Kanakaraju *et al*. (2015) and Montes *et al*. (2016), in which, at deprotonated form the naproxen is oxidized and, after that, a decarboxylation reaction takes place. The uncharged radical formed –hence, lower influence of the pH in this case- is oxidized involving the formation of a cation that is further stabilized.

Reaction mechanism

The liquid medium was analysed by LC-MS after each experiments at different reaction times, in order to identify the reaction products. From the TOC analysis previously shown, it was observed that the NPX of the solution was mineralized in an important extent, so identification of reaction products, previous to total degradation could give information about the reactions pathway. Four reaction intermediates were detected by means of exact mass measurements (m/z of 148, 166, 186 and 202). The m/z=202 was detected in all samples, whereas the other compounds were just detected during the first 10 h of reaction in the case of the degradation experiment under fix potential. This fact suggests their complete degradation after this time, which is consistent to the TOC results obtained, or that they are present at very low concentration.

With these premises, Figure 7 presents the proposed pathway for the NPX degradation by electroxidation. As it was previously mentioned, the reaction would initiate with the oxidation of the deprotonated form of naproxen molecule following the detailed mechanism of Kanakaraju *et al*. (2015) and Montes *et al*. (2016), yielding 2-acetyl-6-methoxynaphtalene (compound 1), with m/z = 200, as well as 2-(1-hydroxyethyl)-6-methoxynaphthalene

305 (compound 2), with m/z=202, compound detected in all analysed samples. Likewise, it was
306 described the formation of strong oxidants such as active chlorine species and hydroxyl
307 radicals (·OH). Active chlorine species, mainly chlorine and hypochlorite, can be generated
308 from direct oxidation of the chlorine ion, present in the solution from the NaCl and KCl present
309 in the phosphate buffer (Candia-Onfray *et al*. 2018). The electrolysis of aqueous solution in
310 presence of chlorides could oxidize the reactant to different oxo-chlorinated compounds, but
311 any of these compounds were here detected. Likewise, by anodic discharge of water, ·OH
312 radicals which could react either with the reactant or with the intermediates molecules can
313 follow the oxidation reactions (Hamza *et al*., 2011). In this way, the ionized molecule formed
314 after the second one-electron transfer, could be readily attacked by the electrophilic ·OH and
315 rapidly oxidized (Kuo-Lin Huang 2017). The radical oxidation from the intermediate products is
316 corroborated by the fact that NPX degradation is higher than TOC removal at both stirring
317 speeds and, add to this, the mass transfer limitation influences mainly this electrochemical
318 oxidation, since the NPX removal difference between both speeds (82.5 – 77 %) double the
319 TOC degradation interval (70 – 67 %). This oxidation would yield 1-(6-hydroxynaphthalen-2-
320 yl)ethanone, m/z = 186 (compound 3), which can be hydroxylated to compound 4, m/z=203.
321 Further degradation of the above mentioned compounds would open an aromatic ring, giving
322 the phthalic acid, m/z=166 (compound 5) and m-vinylbenzoic acid m/z= 148 (compound 6),
323 which are finally oxidized to CO_2 and H_2O. This oxidation steps from compound 3 to
324 compounds 5 and 6 were already proposed by Coria at al. (2016) in the degradation of NPX by
325 Fenton advanced oxidation and by Wang *et al*. (2018) in the degradation by photocatalysis;
326 whereas the final oxidation steps from the open benzoic rings were observed in the
327 paracetamol electrooxidation by Periyasamy and Muthuchamy (2018). The formation of the
328 acidic species in the ring openings justify the decrease in the medium pH with the advanced of
329 the reaction observed by Chin *et al*. (2014) under uncontrolled pH conditions. Likewise, it is
330 remarkable that hydroxyl radicals could be also formed by oxidation of the oxygen molecule,

and further decomposition of the hydrogen peroxide formed, being probably this reaction inhibit in acid medium (Periyasamy and Muthuchamy 2018).

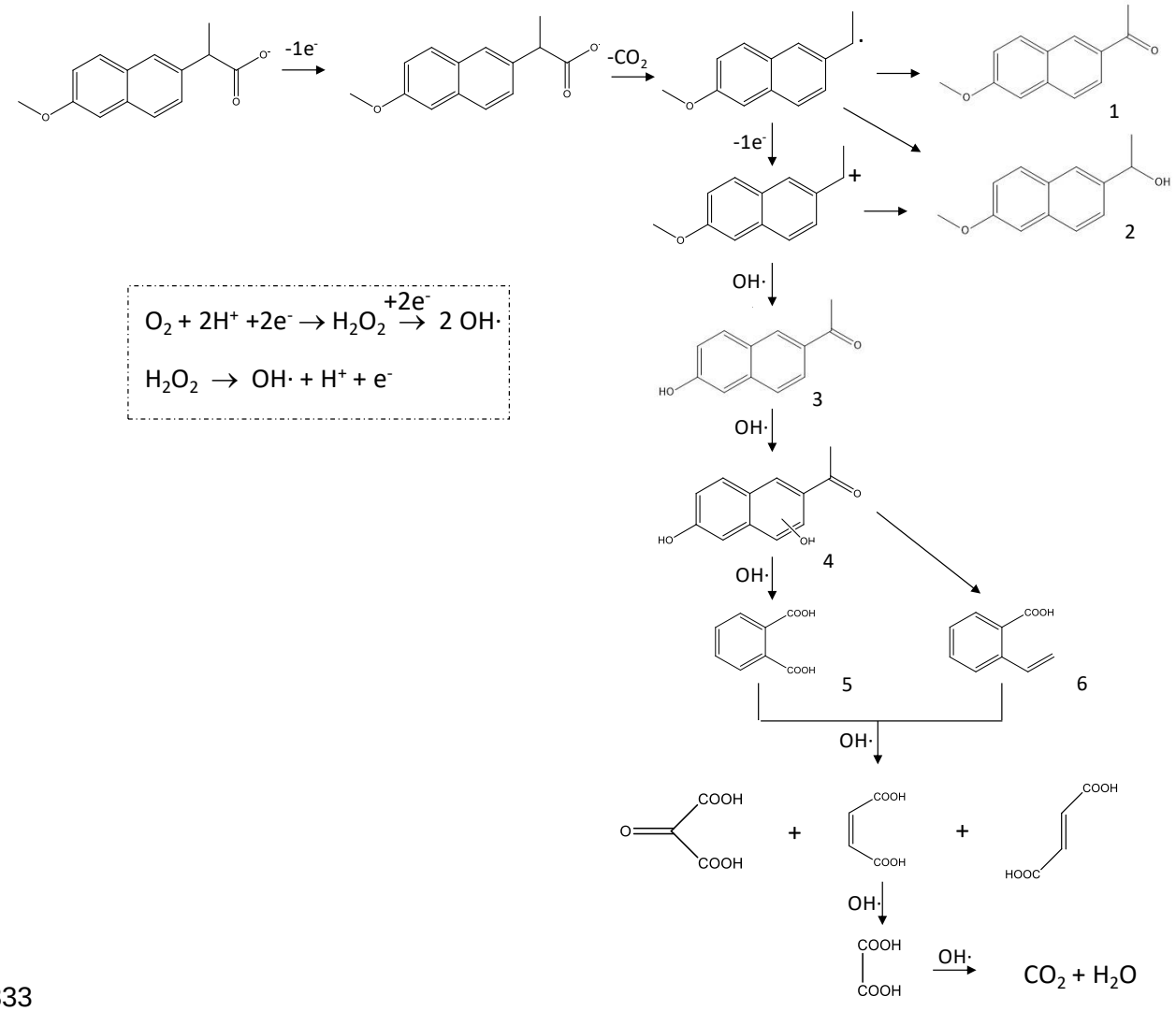

Figure 7. Proposed electrochemical degradation pathway of NPX.

CONCLUSIONS

Naproxen degradation by cyclic voltammetry, and three different MWCNT working electrodes (MWCNT, MWCNT-COOH and MWCNT-NH_2), was studied. Electrochemical oxidation leads to two oxidation peaks compatible with the oxidation of deprotonated NPX, followed by decarboxylation and further electron transfer oxidation. The mass transfer limits the process as it was deduced from experiences at different scan rates, as well as by the NPX degradation under 500 and 250 rpm stirring speed. In this way, the maximum removal efficiency (82.5%) was reached at constant potential (+1.5V) after 20 hours at 500 rpm. TOC analysis confirm the Naproxen degradation since $TOC/TOC_0 < 30\%$ was obtained.

From experiments in the pH range 5-11 it was observed that degradation is favoured at low pH due to the interaction between deprotonated form of the reactant and the surface. Therefore, MWCNT-NH_2, with the highest isoelectric point (4.70) is the most promising material. Further oxidation, carried out on the ionized molecule seems to be more favourable on the MWCNT-COOH material. Subsequent oxidation steps, until mineralization of the NPX, and based on degradation byproducts analysed by LC-MS, are attributed mainly to ·OH.

Acknowledgements

This work was supported by the Spanish Government (contract CTQ2011-29272-C04-02). Y. Patiño acknowledges the Government of the Principality of Asturias for a Ph.D. fellowship (Severo Ochoa Program).

References

Aguilar-Lira, G.Y., Álvarez-Romero, G.A., Rojas-Hernández, A., Páez-Hernández, M.E., Rodríguez-Ávila, J.A. & Romero-Romo, M.A. 2015 New insights on Naproxen quantification using voltammetry and graphite electrodes: development of an optimized and competitive methodology. *ECS Transactions,* **64**, 79-89.

Ardelean, M., Manea, F., Pop, A. & Schoonma, J. 2016 Carbon-Based Electrochemical Detection of Pharmaceuticals from Water. *International Journal of Environmental and ecological Engineering* **10**, 1237-1242.

Candia-Onfray, C., Espinoza, N., Sabino da Silva, E.B.,Toledo-Neira, C., Espinoza, L.C., Santander, R., García, V. & Salazar, R. 2018 Treatment of winery wastewater by anodic oxidation using BDD electrode. *Chemosphere* **206**, 709-717.

Chin, C.-J.M., Chen, T.-Y., Lee, M., Chang, C.-F., Liu, Y.-T. & Kuo, Y.-T. 2014 Effective anodic oxidation of naproxen by platinum nanoparticles coated FTO glass. *Journal of Hazardous Materials* **277**, 110-119.

Coria, G., Sirés, I., Brillas, E. & Nava, J.L. 2016 Influence of the anode material on the degradation of naproxen by Fenton-based electrochemical processes. *Chemical Engineering Journal* **304**, 817-825.

Ding, T., Lin, K., Yang, B., Yang, M., Li, J., Li, W. & Gan, J. 2017 Biodegradation of naproxen by freshwater algae Cymbella sp. and Scenedesmus quadricauda and the comparative toxicity. *Bioresource Technology* **238**, 164-173.

Hamza, M., Ammar, S. & Abdelhédi, R. 2011 Electrochemical oxidation of 1,3,5-trimethoxybenzene in aqueous solutions at gold oxide and lead dioxide electrodes. *Electrochimica Acta* **56**, 3785-3789.

Huang, K.-L., Chu, Y.-C., Chen, H.-R. & Kuo, Y.-M. 2017 Electrochemical degradation od Bisphenol A in water with/without Ce(IV) addition. *International Journal of Electrochemical Science* **12**, 12098-12111.

Jain, R. & Sharma, S. 2012 Glassy carbon electrode modified with multi-walled carbon nanotubes sensor for the quantification of antihistamine drug pheniramine in solubilized systems. *Journal of Pharmaceutical Analysis* **2**, 56-61.

Kanakaraju, D., Motti, C.A., Glass, B.D. & Oelgemöller, M. 2015 TiO_2 photocatalysis of naproxen: Effect of the water matrix, anions and diclofenac on degratation rates. *Chemosphere* **139**, 579-588.

Katsigiannis, A., Noutsopoulos, C., Mantziaras, J., Gioldasi, M. 2015 Removal of emerging pollutants through granular activated carbon. *Chemical Engineering Journal* **280**, 49-57.

Kumar, L., Suhas, B. S., Girish Pai, K., & Verma, R. 2015 Determination of saturated solubility of naproxen using UV visible spectrophotometer. *Research Journal of Pharmacy and Technology* **8**, 825-828.

Loss, R., Carvalho, R., Antonio, D.C., Comero, S., Locoro, G., Tavazzi, S., Paracchini, B., Ghiani, M., Lettieri, T., Blaha, L., Jarosova, B., Voorspoels, S., Servaes, K., Haglund, P., Fick, J., Lindberg, R.H., Schwesig, D. & Gawlik, B.M. 2013 EU-wide monitoring survey on emerging polar organic contaminants in wastewater treatment plant effluents. *Water Research* **47**, 6475-6487.

Montes, H.O., Lima, A. P., Cunha, R.R., Guedes, T.J., dos Santos, T.P., Nossol, E., Richter, E.M. & Munoz, R.A.A. 2016 Size effects of multi-walles carbon nanotubes on the electrochemical oxidation of propionic acid derivative drugs: ibuprofen and naproxen. *Journal of Electroanalytical Chemistry* **775**, 342-349.

Patiño, Y., Díaz, E., Ordóñez, S., Gallegos-Suarez, E., Guerrero-Ruiz, A. & Rodríguez-Ramos, I. 2015 Adsorption of emerging pollutants on functionalized multiwall carbon nanotubes. *Chemosphere* **136**, 174-180.

Patiño, Y., Pilehvar, S., Díaz, E., Ordóñez, S. & De Wael, K. 2017 Electrochemical reduction of nalidixic acid at glassy carbon electrode modified with multi-walled carbon nanotubes. *Journal of Hazardous Materials* **323**, Part B, 621-631.

Patiño, Y., Díaz, E., Lobo-Castañón, M.J. & Ordóñez, S. 2018 Carbon nanotube modified glassy carbon electrode for electrochemical oxidation of alkylphenol ethoxylate. *Water Science and Technology* **77**, 2436-2444.

Pavlishchuk, V.V. & Addison, A.W. 2000 Conversion constants for redox potentials measured versus different reference electrodes in acetonitrile solutions at 25°C. *Inorganica Chimica Acta* **298**, 97-102.

Periyasamy, S. & Muthuchamy, M. 2018 Electrochemical oxidation of paracetamol in water by graphite anode: Effect of pH, electrolyte concentration and current density. *Journal of Environmental Chemical Engineering* **34**, 503-511.

Sarhangzadeh, K. 2015 Application of multi wall carbon nanotube–graphene hybrid for voltammetric determination of naproxen. *Journal of the Iranian Chemical Society* **12**, 2133-2140.

Shin, H., Song, J., Shin, E. & Kang, C. 2011 Ion-exchange adsorption of copper(II) ions on functionalized single-wall carbon nanotubes immobilized on a glassy carbon electrode. *Electrochimica Acta* **56**, 1082-1088.

Soltani, N., Tavakkoli, N., Mosavimanesh, Z.S., Davar, F. 2018 Electrochemical determination of naproxen in the presence of acetaminophen using carbon paste electrode modified with activated carbon nanoparticles. *Comptes Rendus Chimie* **21**, 54-60.

Štrbac, D., Aggelopoulos, C.A., Štrbac, G., Dimitropoulos, M., Novaković, M., Ivetić, T. & Yannopoulos, S.N. 2018 Photocatalytic degradation of Naproxen and methylene blue: Comparison between ZnO, TiO_2 and their mixture. *Process Safety and Environmental Protection* **113**, 174-183.

Tashkhourian, J., Hemmateenejad, B., Beigizadeh, H., Hosseini-Sarvari, M. & Razmi, Z. 2014 ZnO nanoparticles and multiwalled carbon nanotubes modified carbon paste electrode for determination of naproxen using electrochemical techniques. *Journal of Electroanalytical Chemistry* **714**, 103-108.

Wang, F., Wang, Y., Feng, Y., Zeng, Y., Xie, Z., Zhang, Q., Su, Y., Chen, P., Liu, Y., Yao, K., Lv, W. & Liu, G. 2018 Novel ternary photocatalyst of single atom-dispersed silver and carbon

quantum dots co-loaded with ultrathin g-C3N4 for broad spectrum photocatalytic degradation of naproxen. *Applied Catalysis B: Environmental* **221**, 510-520.

Wojcieszyńska, D., Domaradzka, D., Hupert-Kocurek, K. & Guzik, U. 2014 Bacterial degradation of naproxen – Undisclosed pollutant in the environment. *Journal of Environmental Management* **145**, 157-161.

Wu, J., Wang, W., Wang, M., Liu, H., Pan, H. 2016 Electrochemical behavior and direct quantitative determination of tanshione IIA in micro-emulsion. *Intenational Journal of electrochemical science* **11**, 5165-5179.